[4]Bahar, C., Alemdaroglu, N., Ozyoruk, Y., and Temel, E., "Euler Solutions for a Medium Range Cargo Aircraft," *Journal of Aircraft*, Vol. 40, No. 2, 2003, pp. 393–395.

[5]"CFD-FASTRAN User Manual," ver. 2.2, CFD Research Corp., Huntsville, AL, 1998.

[6]Kurtulus, D. F., "Aerodynamic Analysis of a Medium Range Cargo Aircraft Using a Panel Method," M.S. Thesis, Dept. of Aerospace Engineering, Middle East Technical Univ., Ankara, Turkey, Jan. 2002.

[7]Nathman, J., "VSAERO User's Manual," Analytics Methods Inc., Redmond, WA, 1982.

[8]"CFD-GEOM User Manual," ver. 5, CFD Research Corp., Huntsville, AL, 1998.

[9]Roe, P. L., "Approximate Riemann Solvers, Parameter Vectors and Difference Schemes," *Journal of Computational Physics*, Vol. 43, No. 2, 1981, pp. 357–372.

[10]Van Leer, B., "Flux-Vector Splitting for the Euler Equations," *Lecture Notes in Physics*, Vol. 170, Springer-Verlag, NY, 1982, pp. 507–512.

[11]Baldwin, B. S., and Lomax, H., "Thin Layer Approximation and Algebraic Model for Separated Flows," AIAA Paper 78-257, Jan. 1978.

[12]Speziale, C., Abi, R., and Anderson, E., "A Critical Evaluation of Two-Equation Models for Near-Wall Turbulence," AIAA Paper 90-1481, Jan. 1990.

[13]Wilcox, D. C., "A Half Century Historical Review of the k–ω Model," AIAA Paper 91-0615, Jan. 1991.

[14]Uygun, M., and Tuncer, I. H., "A Computational Study of Subsonic Flows over a Medium Range Cargo Aircraft," AIAA Paper 2003-3661, June 2003.

Effects of Flow Separation on Aerodynamic Loads in Linearized Thin Airfoil Theory

A. Khrabrov*
TsAGI, Russia
and
M. Ol†
U.S. Air Force Research Laboratory, Wright–Patterson Air Force Base, Ohio 45433-7542

Introduction

In various problems of modeling steady and unsteady aerodynamic loads, it is useful to know the explicit dependence of the loads on the airfoil upper-surface separation point location, for example, see Ref. 1. We consider an approach based on classical thin airfoil theory, for symmetrical airfoils at small angles of attack, that is, inclined flat plates.[2–4] A separated region in an ideal fluid is modeled as a semi-infinite zone of uniform pressure with Kirchhoff's free streamline boundaries, originating from a prescribed location on the airfoil upper surface and from the trailing edge. A closed-form solution for lift and pitching moment coefficient is obtained by assuming small angles of attack and thin separated regions, thus allowing linearization.

The linear solution is obtained in singular integral form.[5] It is then compared to the Chaplygin and Lavrentiev classical solution[6] and an XFOIL solution[7,8] for a NACA 0012 airfoil.

Received 14 October 2003; revision received 19 January 2004; accepted for publication 20 January 2004.

*Chief, Unsteady Aerodynamics Branch, Central Aerohydrodynamics Institute; khrabrov@postman.ru.

†Aerospace Engineer, Air Vehicles Directorate, Aeronautical Sciences Division; Michael.Ol@wpafb.af.mil. Member AIAA.

Linear Thin Airfoil Theory with Flow Separation

The flowfield in the physical plane is shown in Fig. 1a. To make the problem dimensionless, the airfoil has unit chord and the velocity at infinity is a vector of unit magnitude. Free streamlines emanate from the airfoil trailing edge and the upper-surface separation point. On these streamlines, the pressure is uniform and equal to the value at infinity. The difficult task of determining the geometry of these streamlines is circumvented in the linear approximation, where the respective boundary conditions can be enforced on the Ox axis.

Because the vorticity vanishes everywhere except on the airfoil boundary and the free streamlines, the velocity field has a potential. When the boundary-value problem is posed in terms of the disturbance potential φ, the boundary conditions become no through-flow on the wetted portion of the airfoil, uniform pressure on the boundaries of the separated zone (equivalent to zero streamwise component of disturbance velocity), finite velocity at both separation points, and the disturbance potential decaying to zero at infinity:

$$\begin{aligned}
\triangle\varphi &= 0 \\
\varphi_y &= V(x), \qquad 0 < x < x_s, \qquad y = +0 \\
\varphi_y &= V(x), \qquad 0 < x < 1, \qquad y = -0 \\
\varphi_x &= 0, \qquad x_s < x < \infty, \qquad y = +0 \\
\varphi_x &= 0, \qquad 1 < x < \infty, \qquad y = -0 \\
\varphi_x &< \infty, \qquad x = x_s, \qquad y = +0 \\
\varphi_x &< \infty, \qquad x = 1, \qquad y = -0 \\
\varphi &\to 0, \qquad x^2 + y^2 \to \infty
\end{aligned} \tag{1}$$

$V(x)$ is known on the wetted portion of the airfoil, as a function of angle of attack and airfoil shape. Appealing to complex variables theory, we introduce the complex flow potential W, and seek the complex conjugate disturbance velocity $\mathrm{d}W/\mathrm{d}z = U - iV$, where $U = \varphi_x$ and $V = \varphi_y$. We use the conformal mapping $\zeta = \sqrt{z}$, which maps the physical plane $z = x + iy$ with branch cut along the positive side of the real axis, corresponding to the airfoil and separated zone, onto the upper-half of the image plane, $\zeta = \xi + i\eta$ (Fig. 1). The complex conjugate velocities in the two planes are related through

$$\frac{\mathrm{d}W}{\mathrm{d}z} = \frac{\mathrm{d}W/\mathrm{d}\zeta}{\mathrm{d}z/\mathrm{d}\zeta} = \frac{1}{2\zeta}\frac{\mathrm{d}W}{\mathrm{d}\zeta}$$

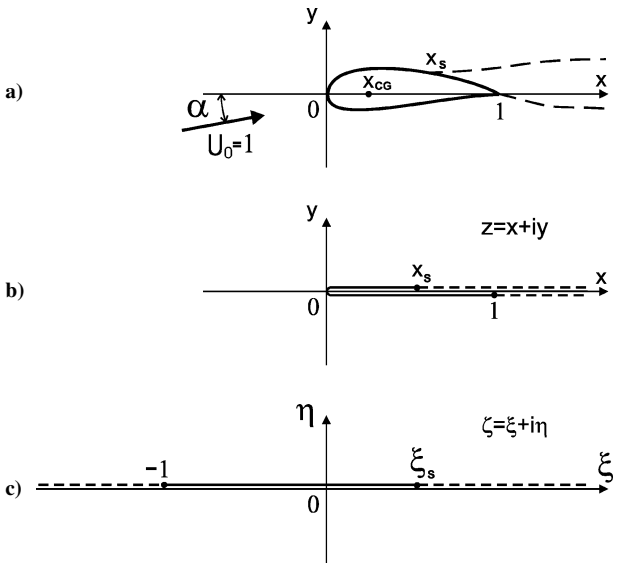

Fig. 1 Schematic for flow about a thin airfoil with upper-surface separation, in a) the linear approximation, b) the physical plane $z = x + iy$, and c) the image plane $\zeta = \xi + i\eta$.

from which we obtain the following relation between the disturbance velocity components in the ζ plane with $\eta = 0$ and the z plane on the airfoil and the separated region:

$$u(\xi) = 2\xi U, \qquad v(\xi) = 2\xi V \tag{2}$$

Thus, in the ζ plane, we have a boundary-value problem for the harmonic function $\mathrm{d}W/\mathrm{d}\zeta$, where on one portion of the real axis, $-\infty < \xi < -1$ and $\xi_s < \xi < \infty$, the real part of the function $u(\xi) = 0$ is given, and on the other portion, $-1 < \xi < \xi_s$, its imaginary part, $v(\xi)$, is given.

Following Refs. 2 and 5, the solution of this boundary-value problem can be written as the singular integral,

$$\frac{\mathrm{d}W}{\mathrm{d}\zeta} = \frac{1}{i\pi}\sqrt{(\zeta+1)(\zeta-\xi_s)}\int_{-1}^{\xi_s}\frac{v(s)\,\mathrm{d}s}{(s-\zeta)\sqrt{(s+1)(\xi_s-s)}} \tag{3}$$

from which the airfoil velocity distribution can be expressed in the form

$$u(\xi) = \frac{1}{\pi}\sqrt{(\xi+1)(\xi_s-\xi)}\int_{-1}^{\xi_s}\frac{v(s)\mathrm{d}s}{(s-\xi)\sqrt{(s+1)(\xi_s-s)}} \tag{4}$$

For separated flow about a symmetric airfoil at an angle of attack greater than the dimensionless airfoil thickness, the dominant term in the vertical velocity component at the airfoil boundary is

$$V(x) = -\alpha$$

in the physical plane, and

$$v(\xi) = -2\alpha\xi \tag{5}$$

in the image plane.

Substituting this value into expression (4), we obtain

$$u(\xi) = -\frac{2\alpha}{\pi}\sqrt{(\xi+1)(\xi_s-\xi)}\int_{-1}^{\xi_s}\frac{s\,\mathrm{d}s}{(s-\xi)\sqrt{(s+1)(\xi_s-s)}}$$

for the disturbance velocity horizontal component at the airfoil boundary.

When the definite integral

$$\int_{-1}^{\xi_s}\frac{s\,\mathrm{d}s}{(s-\xi)\sqrt{(s+1)(\xi_s-s)}} = \pi$$

is evaluated, the final expression for the disturbance velocity in the image plane becomes

$$u(\xi) = -2\alpha\sqrt{(\xi+1)(\xi_s-\xi)} \tag{6}$$

which is linear in angle of attack and nonlinear in upper-surface separation point location, $\xi_s = \sqrt{x_s}$.

The normal force and pitching moment coefficients are found from the velocity distributions. In the physical plane we have

$$C_N = 2\int_0^1 (C_{p-} - C_{p+})\,\mathrm{d}x$$

$$C_m = -2\int_0^1 (C_{p-} - C_{p+})(x - x_{\mathrm{CG}})\,\mathrm{d}x \tag{7}$$

Here x_{CG} is the reference point for pitching moment coefficient. The plus and minus subscripts refer to the upper and lower airfoil surfaces, respectively, and the pressure coefficient C_p is

$$C_p = (p - p_\infty)/\rho = -U(x) = -u(\xi)/2\xi$$

Integrate along the airfoil in the image plane ζ, then

$$C_N = -2\int_{-1}^{\xi_s} u(\xi)\,\mathrm{d}\xi, \qquad C_m = -2\int_{-1}^{\xi_s}\xi^2 u(\xi)\,\mathrm{d}\xi - x_{\mathrm{CG}}C_N \tag{8}$$

Substitute the expressions for velocity distribution (6), then

$$C_N = 4\alpha\int_{-1}^{\xi_s}\sqrt{(\xi+1)(\xi_s-\xi)}\,\mathrm{d}\xi$$

$$C_m = -4\alpha\int_{-1}^{\xi_s}\xi^2\sqrt{(\xi+1)(\xi_s-\xi)}\,\mathrm{d}\xi - x_{\mathrm{CG}}C_N$$

The integrals on the right hand side evaluate to

$$\int_{-1}^{\xi_s}\sqrt{(\xi+1)(\xi_s-\xi)}\,\mathrm{d}\xi = \pi(\xi_s+1)^2$$

$$\int_{-1}^{\xi_s}\xi^2\sqrt{(\xi+1)(\xi_s-\xi)}\,\mathrm{d}\xi = \frac{5\pi}{128}\left(\xi_s^2-1\right)^2 + \frac{\pi}{3}\xi_s(\xi_s+1)^2$$

Thus, we obtain

$$C_N = (\pi/2)\alpha(1+\xi_s)^2$$

$$C_m = -(\pi/32)\alpha(1+\xi_s)^2\left(5 - 6\xi_s + 5\xi_s^2 - 16x_{\mathrm{CG}}\right) \tag{9}$$

These formulas give the explicit effect of separation point location on the airfoil lift and pitching moment, in the linear approximation. Also note that the expressions for C_N were obtained earlier by other means in Refs. 3 and 4. In fully attached flow ($x_s = 1$, $\xi_s = 1$), the usual relations for thin airfoils are recovered:

$$C_N = 2\pi\alpha, \qquad C_m = -2\pi\alpha\left(\tfrac{1}{4} - x_{\mathrm{CG}}\right)$$

Nonlinear Model for Separated Flow About an Airfoil

The preceding main simplifying assumptions were that the zone of separated flow is thin and that its boundary conditions can instead be enforced on the longitudinal axis. We now examine the error in velocimetry distribution and aerodynamic loads introduced by this simplification.

In 1933, Chaplygin and Lavrentiev[6] solved the nonlinear problem of separated two-dimensional irrotational incompressible flow about a flat plate with trailing-edge separation. The separated zone was also modeled as an infinite Kirchhoff zone. The angle of attack can take on arbitrarily large values, and the boundary conditions on the boundary of the separated region are not projected onto the x axis, but are enforced on the physical boundary of the separated region, whose geometry is ascertained as part of the solution.[6]

A schematic is given in the Fig. 2a. The plate BD has length of unity, and freestream $U_0 = 1$, also of unity magnitude, is inclined at infinity at some arbitrary angle α to the plate. The point A on the plate's lower surface is the stagnation point. Separation occurs at point C on the upper surface, forming the free boundary CE, on which the pressure is uniform and equal to the value at infinity. The shape of the CE curve is determined as part of the solution. Separation on the lower surface occurs at point D, the airfoil trailing edge. DE is likewise a free boundary, whose shape is to be determined.

The domain of the complex flow potential $W = \Phi + i\Psi$ is a plane with branch cut along the positive real axis (Fig. 2b). The problem is solved with the help of a conformal mapping that maps the first quadrant of the plane with the image variable ζ (Fig. 2) onto the region where the complex potential W and complex velocity $\mathrm{d}W/\mathrm{d}z$ vary. Corresponding points in the two planes are denoted as follows: $\zeta = \mu$ corresponds to the critical point A in the plane ζ, $\zeta = \nu$ corresponds to the plate leading edge B, and $\zeta = i$ corresponds to point E, infinitely distant. The function $W(\zeta)$ has a second-order zero at point A and a second-order pole at E. When the function $W(\zeta)$ is continued onto the entire ζ plane using the symmetry principle, $W(\zeta)$ likewise has a second-order zero at $\zeta = -\mu$ and a second-order pole at $\zeta = -i$. From these singularities one can find that

$$W(\zeta) = N[(\zeta^2 - \mu^2)/(\zeta^2 + 1)]^2 \tag{10}$$

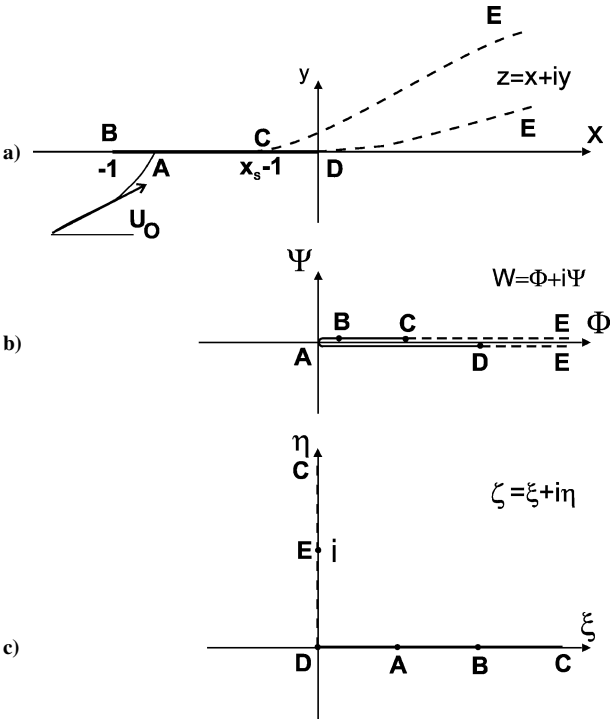

Fig. 2 Schematic for flow about a plate with upper-surface separation in the Chaplygin–Lavrentiev problem, in a) the $z = x + iy$ plane, b) the complex potential plane $W = \Phi + i\Psi$, and c) the image plane $\zeta = \xi + i\eta$

where N is some real constant. When Eq.(10) is differentiated,

$$\frac{\mathrm{d}W}{\mathrm{d}\zeta} = a\frac{\zeta(\zeta^2 - \mu^2)}{(\zeta^2 + 1)^3} \tag{11}$$

where the notation $a = 4N(1 + \mu^2)$ is introduced.

Analogous consideration of the singularities of $\mathrm{d}W/\mathrm{d}z$ in the ζ plane, using the symmetry principle and the fact that $\mathrm{d}W/\mathrm{d}z = 1$ at infinity, led the authors[6] to conclude that

$$\frac{\mathrm{d}W}{\mathrm{d}z} = \frac{(\zeta - \mu)(\zeta + \nu)}{(\zeta + \mu)(\zeta - \nu)} \tag{12}$$

From this relation, one can solve for the unknown constants μ and ν and the inclination angle of the freestream at infinity. We introduce the notation $k = \tan\alpha/2$. When $\zeta = i$ is substituted into Eq. (12),

$$k = (\nu - \mu)/(1 + \mu\nu) \tag{13}$$

When Eqs. (11) and (12) are compared,

$$\frac{\mathrm{d}z}{\mathrm{d}\zeta} = a\frac{\zeta(\zeta + \mu^2)^2(\zeta - \nu)}{(\zeta - \nu)(\zeta^2 + 1)^3} \tag{14}$$

This is a differential relation between the z and ζ planes. Chaplygin and Lavrentíiev expanded (14) into partial fractions, and noting that $z = 0$ when $\zeta = 0$, integrated and obtained the final form of the mapping from the image plane ζ onto the physical plane z:

$$\frac{z}{a} = \frac{C\zeta - B}{4(\zeta^2 + 1)^2} + \frac{(3C + 4E)\zeta - 4D}{8(\zeta^2 + 1)} + \left(\frac{3}{8}C + \frac{E}{2} + H\right)\arctan\,\zeta + \frac{F}{2}\,\ell_n\frac{\nu^2(\zeta^2 + 1)}{(\zeta + \nu)^2} + \frac{B}{4} + \frac{D}{2} \tag{15}$$

where the coefficients B, C, D, E, F, and H are expressed in terms of k and ν:

$$B = -\frac{(1 - k^2)(1 + \nu^2)}{(1 + k\nu)^2}, \qquad C = \frac{2k(1 + \nu^2)}{(1 + k\nu)^2}$$

$$D = \frac{1 + 2k\nu - k^2\nu^2}{(1 + k\nu)^2}, \qquad E = -\frac{2k(1 + k\nu + \nu^2)}{(1 + k\nu)^2}$$

$$F = -\frac{2k^2\nu^2}{(1 + \nu^2)(1 + k\nu)^2}, \qquad H = \frac{2k^2\nu^3}{(1 + \nu^2)(1 + k\nu)^2}$$

Because the airfoil leading edge $z = -1$ (point B) corresponds to the point $\zeta = \nu$, an expression for the unknown real coefficient a can be found. From Eq. (15) we get

$$-\frac{1}{a} = \frac{C\nu - B}{4(\nu^2 + 1)^2} + \frac{(3C + 4E)\nu - 4D}{8(\nu^2 + 1)} + \left(\frac{3}{8}C + \frac{E}{2} + H\right)\arctan\,\nu + \frac{F}{2}\,\ell_n\frac{(\nu^2 + 1)}{4} + \frac{B}{4} + \frac{D}{2} \tag{16}$$

An analogous relation for C ($\zeta = \infty$, $z = x_s - 1$) gives

$$(x_s - 1)/a = (\pi/2)\left[\tfrac{3}{8}C + E/2 + H\right] + F\,\ell_n\nu + B/4 + D/2 \tag{17}$$

For given values of k and x_s, the preceding expressions can be considered as nonlinear equations for ν. The quantity a in this expression is explicitly found from k and ν, with the help of Eq. (16).

Lacking computers, Chaplygin and Lavrentiev obtained approximate solutions, but only for three values of angle of attack (5, 10, and 15 deg) and for two or three separation point locations for each angle. However today, a numerical solution of the nonlinear equation (17) is straightforward.

Computations where organized as follows: the angle of attack (parameter k) and location of separation on the plate upper surface (x_s) are prescribed. Equation (17) is solved numerically for the parameter ν. Then the parameter μ is found from

$$\mu = (\nu - k)/(1 + k\nu) \tag{18}$$

which immediately follows from Eq. (13). This means that the problem has now been solved in parametric form. For example, with the help of relation (15), specifying a $\zeta \in (0, i)$ gives the shape of the streamline DE, and specifying a $\zeta \in (i, i\infty)$ gives the shape of the free streamline CE, emanating from the airfoil upper surface.

The nondimensional flow speed at the plate is then given by

$$U = \frac{(\zeta - \mu)(\zeta + \nu)}{(\zeta + \mu)(\zeta - \nu)} \tag{19}$$

which follows from formula (11) for the upper surface if we take $\zeta \in (\nu, \infty)$ and for the lower surface if $\zeta \in (0, \nu)$.

In Ref. 6, the dimensionless total force on the plate with separation is given as

$$C_\tau + iC_N = -i\oint \mathrm{d}z \tag{20}$$

where the contour integral is taken around the point at infinity, which corresponds to the point E ($\zeta = i$) in the image plane ζ. With the help of expression (15), this integral is readily evaluated:

$$C_\tau + iC_N = \pi a\left[F - i\left(\tfrac{3}{8}C + \tfrac{1}{2}E + H\right)\right] \tag{21}$$

Thus, after the numerical solution of the problem and evaluation of the parameter ν, one can calculate the loading on the plate.

Calculation of the pitching moment is somewhat more involved. The authors[6] did not consider this question. We compute the pitching moment numerically from the velocity distribution (19). Along with C_m, one can also numerically integrate to find C_N and compare that with the analytical result (21). Discretization of the airfoil surface was considered satisfactory when the numerically computed C_N differed from the analytical value by no more than 2–3%.

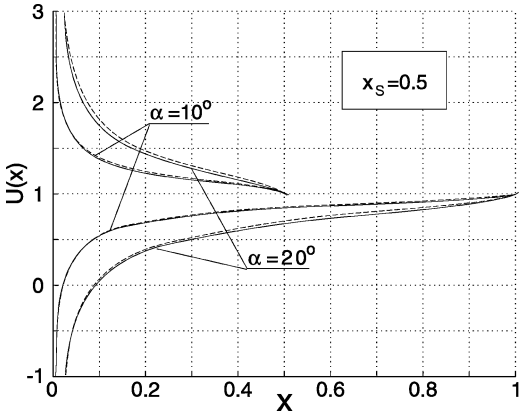

Fig. 3 Airfoil velocity distributions at $\alpha = 10$ and 20 deg with flow separation at $x_s = 0.5$: – – –, linear approach and ——, nonlinear approach.

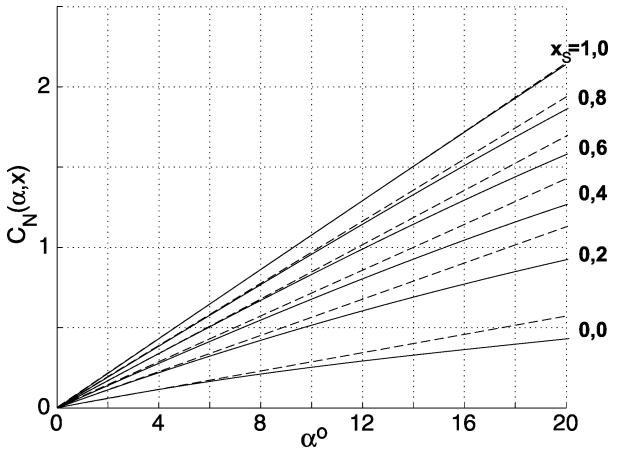

Fig. 4 Variation of normal force coefficient with angle of attack α for different values of upper-surface separation point x_s: – – –, linear theory and ——, nonlinear theory.

Comparison of Linear and Nonlinear Theories

Figure 3 shows airfoil velocity distributions with upper-surface separation onset at $x_s = 0.5$, for $\alpha = 10$ and $\alpha = 20$ deg. Solid lines indicate results obtained from formula (19) and dashed lines from linear theory (6). Formula (6) gives the disturbance velocity, Whereas Eq. (19) is for the total velocity distribution. I herefore, for comparison purposes, a freestream velocity of $U_0 = 1$ was added to the linear-theory result. For $\alpha = 10$ deg, the linear and nonlinear results are practically identical. Agreement is worse at $\alpha = 20$ deg, but the simple linear theory still captures the trend of the Chaplygin–Lavrentiev solution.

In Fig. 4, the solid lines denote the Chaplygin–Lavrentiev results for C_N, in the angle-of-attack range of $\alpha = 0$–20 deg, for upper-surface separation point locations of $x_s = 0$, 0.2, 0.4, 0.6, 0.8, and 1.0. Dashed lines show the corresponding linear theory results. The linear theory somewhat overpredicts C_N, with the discrepancy increasing with increasing size of the separated region.

For $x_s = 0$ (leading-edge separation), the Chaplygin–Lavrentiev solution matches the classical Rayleigh solution[9] for an inclined plate with separation from sharp leading and trailing edges. In modeling a Kirchhoff separated region, Rayleigh obtained the following expression for normal force coefficient:

$$C_N = \frac{2\pi \sin\alpha}{4 + \pi \sin\alpha} \tag{22}$$

Figure 5 shows pitching moment coefficient C_m taken about the point $x_{CG} = 0.25$, as a function of angle of attack α and upper-surface separation point location x_s. Linear-theory results given by formula (9) are in Fig. 5a, Whereas results from numerical integration of the Chaplygin–Lavrentiev pressure distribution are in Fig. 5b. At least qualitatively, the agreement between the two is good.

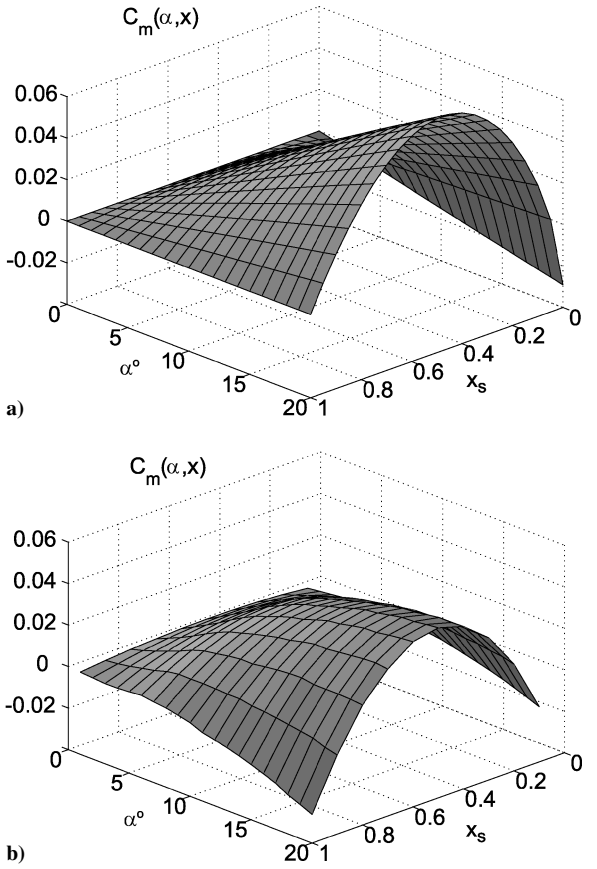

Fig. 5 Comparison of pitching moment coefficient, taken about $x_{CG} = 0.25$, for various values of α and x_s: a) linear theory and b) nonlinear theory.

Comparison of Analytic and Computational Results for Airfoil in Separated Flow

XFOIL, as a representative of modern airfoil codes, was applied to the test case of a NACA 0012 airfoil in the angle-of-attack range $\alpha = 0$–19 deg at $M = 0.15$ and $Re = 1 \times 10^6$. These conditions were deemed typical of experimental conditions in moderate-scale subsonic wind tunnels. The mentioned linear and nonlinear theories require the specification of how the upper-surface separation point varies with angle of attack. The separation point location was taken as the point where the skin-friction coefficient C_f vanishes, according to XFOIL's integral boundary-layer calculation. A leading-edge separation bubble can produce a pocket near the leading edge where $C_f < 0$, but at $Re = 1 \times 10^6$, this does not in general lead to an open separation region, because transition in the free shear layer generally leads to turbulent reattachment.

Calculated results for the NACA 0012 airfoil for separation point locations $x_s(\alpha)$ are given in the lower part of Fig. 6. Normal force and pitching moment coefficients are given in the upper part of Fig. 6. The pitching moment reference point was $x_{CG} = 0.25$. XFOIL results are the solid lines 1 with open circles. Steps in angle of attack were $\Delta\alpha = 0.1$ deg at the higher angles of attack. Solid lines 2 are the calculated nonlinear theory results for $C_N(\alpha)$ and $C_m(\alpha)$, and dashed lines 3 are the linear theory results, given by formula (9). The relation $x_s(\alpha)$ was used to obtain both the linear and nonlinear analytic results.

Nonlinear behavior of the calculated normal force coefficient C_N in the angle-of-attack range $\alpha = 6$–8 deg is due to a laminar separation bubble near the leading edge, for which neither the linear nor the nonlinear analytic theories can account. At large angles of attack, $\alpha > 12$ deg, growth of trailing-edge separation also leads to

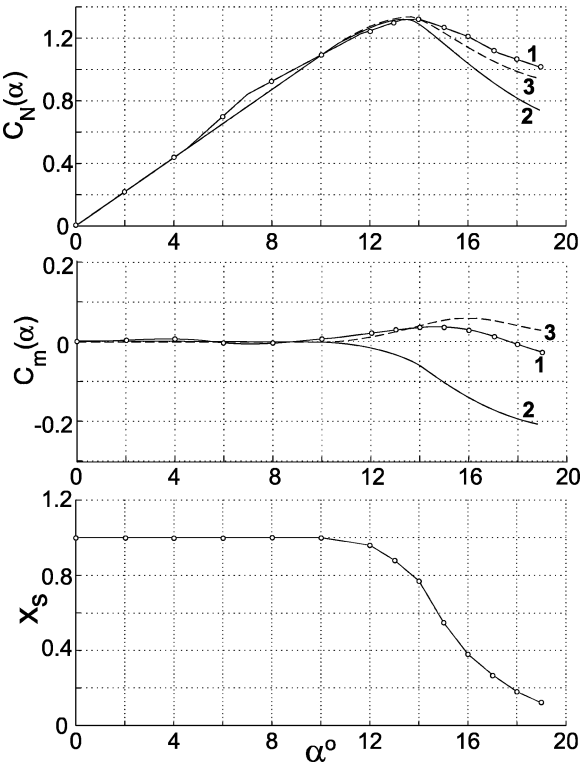

Fig. 6 Comparison of results for separated flow for NACA 0012 airfoil for $M = 0.15$ and $Re = 1 \times 10^6$ using XFOIL (1), the nonlinear theory (2), and the linear theory (3). In (2) and (3) the separation point location $x_s(\alpha)$ was prescribed from XFOIL output (lower part of the figure).

nonlinear behavior in $C_N(\alpha)$ and $C_m(\alpha)$. The linear and nonlinear analytic methods are in reasonable qualitative agreement with the XFOIL prediction of this nonlinear variation. Interestingly, the linear results happen to be in closer agreement with XFOIL than the nonlinear. Evidently, errors due to absence of airfoil thickness and the projection of boundary conditions onto the longitudinal axis to some extent cancel one another.

Conclusions

A solution, linear in angle of attack, is given for flow about a thin symmetric airfoil, that is, an inclined flat plate, with a semi-infinite separated region. This solution allows one to ascertain explicitly the effect of the development of upper-surface separation on the airfoil lift and pitching moment coefficients. The main drawback is the enforcement of the uniform-pressure boundary condition on the corresponding segments of the real axis, rather than on the actual boundary of the separated region. Physically, this assumes that the separated region is thin. Errors resulting from such an approximation were estimated by a comparison with the Chaplygin–Lavrientiev classical nonlinear solution. The linear solution was also compared with XFOIL results for a NACA 0012 airfoil. XFOIL's prediction of the location of the upper surface separation point was input into the analytic solutions, to obtain the static dependency of lift and pitching moment coefficients on angle of attack. Results from the linear and nonlinear analytic solution and the XFOIL computation were in satisfactory agreement.

Acknowledgments

Analytical investigations of airfoil flow separation with linear and nonlinear theories were supported by the Russian Federation Basic Research foundation RFBR Project 03–01–00918.

References

[1]Goman, M. G., and Khrabrov, A. N., "State-Space Representation of Aerodynamic Characteristics of an Aircraft at High Angles of Attack," *Journal of Aircraft*, 1994, Vol. 31, No. 5, pp. 1109–1115.

[2]Sedov, L. I., *Two Dimensional Problems in Hydrodynamics and Aerodynamics*, Wiley, New York, 1965, Chap. 2.

[3]Thwaites, B. (ed.), *Incompressible Aerodynamics*, Dover Publications, Mineola, NY, 1987.

[4]Woods, L. C., *The Theory of Subsonic Plane Flow*, Cambridge Univ. Press, Cambridge, England, U.K., 1961.

[5]Muskhelishvili, N. I., *Singular Integral Equations*, Noordhoff, Groningen, The Netherlands, 1953.

[6]Chaplygin, S. A., and Lavrentiev, A. L., "On the Lift and Drag of a Flat Wing of Infinite Span (Assuming Discontinuous Flow on its Upper Surface)," *Transactions of Central Aerohydrodynamics Institute*, No. 123, 1933.

[7]Drela, M., and Giles, M. B., "Viscous–Inviscid Analysis of Transonic and Low Reynolds Number Airfoils," *AIAA Journal*, Vol. 25, No. 10, 1987 pp. 1347–1355.

[8]Drela, M., "XFOIL: An Analysis and Design System for Low Reynolds Number Airfoils," Conf. on Low Reynolds Number Airfoil Aerodynamics, June 1989.

[9]Rayleigh, "On the Resistance of Fluids," Philosophical Magazine, Vol. 2, Ser. 5, 1876.

Limit-Cycle Oscillations of Swept-Back Trapezoidal Wings at Low Subsonic Flow

Saeed Shokrollahi* and Firooz Bakhtiari-Nejad†
Amirkabir University of Technology, 15875 Tehran, Iran

Introduction

THE effect of sweep angle and taper ratio of swept back trapezoidal wings based on geometrically nonlinear von Kármán plate theory is studied in this Note. A three-dimensional time-domain vortex lattice aerodynamic model is used to investigate the flutter characteristics and limit-cycle oscillations of a low aspect ratio swept back trapezoidal wing at low subsonic flow.

Flutter characteristics and nonlinear response of cantilevered, low-aspect ratio, rectangular and delta wing models in low subsonic flows have been studied recently. Hopkins and Dowell[1] and Weiliang and Dowell[2] studied the limit-cycle oscillations of rectangular cantilever plates in high supersonic flow. Their results provided good physical understanding about the flutter and limit-cycle oscillation characteristics for such plates in a high Mach number supersonic flow. Tang and Dowell[3] and Tang et al.[4] investigated limit-cycle oscillations of cantilever rectangular and delta plates at low subsonic flow. Their analysis included the vortex lattice theory in a reduced-order aerodynamic model. They investigated the effect of a steady angle of attack on both the flutter instability boundary and the limit-cycle oscillations. Bakhtiari-Nejad and Shokrollahi[5] conducted an aeroelastic eigenanalysis of a cantilever plate in low subsonic flow to predict flutter onset. The effect of local forcing functions on the response of a cantilever plate at low subsonic flow was also studied by Bakhtiari-Nejad et al.[6] In that paper, the piezoelectric actuators were used to model the local forcing functions and the effect of their positions on flutter suppression.

Theoretical Development

A plan view schematic diagram of a wing-plate geometry with a three-dimensional vortex lattice model of unsteady flow is shown in

Received 4 May 2003; revision received 1 March 2004; accepted for publication 19 March 2004.

*Ph.D. Student, Department of Mechanical Engineering.
†Associated Professor, Department of Mechanical Engineering.